FAD Is a Preferred Substrate and an Inhibitor of *Escherichia coli* General NAD(P)H:Flavin Oxidoreductase*

Tai Man Louie‡§, Haw Yang¶‖, Pallop Karnchanaphanurach¶, X. Sunney Xie¶, and Luying Xun‡**

From the ‡School of Molecular Biosciences, Washington State University, Pullman, Washington 99164 and ¶Department of Chemistry and Chemical Biology, Harvard University, Cambridge, Massachusetts 02138

Escherichia coli **general NAD(P)H:flavin oxidoreductase (Fre) does not have a bound flavin cofactor; its flavin substrates (riboflavin, FMN, and FAD) are believed to bind to it mainly through the isoalloxazine ring. This interaction was real for riboflavin and FMN, but not for FAD, which bound to Fre much tighter than FMN or riboflavin. Computer simulations of Fre·FAD and Fre·FMN complexes showed that FAD adopted an unusual bent conformation, allowing its ribityl side chain and ADP moiety to form an additional 3.28 H-bonds on average with amino acid residues located in the loop connecting Fβ5 and Fα1 of the flavin-binding domain and at the proposed NAD(P)H-binding site. Experimental data supported the overlapping binding sites of FAD and NAD(P)H. AMP, a known competitive inhibitor with respect to NAD(P)H, decreased the affinity of Fre for FAD. FAD behaved as a mixed-type inhibitor with respect to NADPH. The overlapped binding offers a plausible explanation for the large K_m values of Fre for NADH and NADPH when FAD is the electron acceptor. Although Fre reduces FMN faster than it reduces FAD, it preferentially reduces FAD when both FMN and FAD are present. Our data suggest that FAD is a preferred substrate and an inhibitor, suppressing the activities of Fre at low NADH concentrations.**

Escherichia coli general NAD(P)H:flavin oxidoreductase does not contain any bound flavin cofactor (1, 2). This property separates Fre[1] from the flavin-containing NAD(P)H:flavin oxidoreductases of *Vibrio harveyi* and *V. fischeri* that supply $FMNH_2$ to bacterial luciferases (3, 4). Fre uses either NADH or NADPH as electron donors to reduce FAD, FMN, or riboflavin (Rfl); however, when FAD is the electron acceptor, the K_m

values for NADH and NADPH are exceptionally large (1, 2, 5). Reduced flavins generated by Fre are believed to have important biological functions. It has been shown that the reduced flavins generated by Fre can regulate the activity of the aerobic ribonucleotide reductases by regenerating or scavenging the Tyr^{122} radical of the ribonucleotide reductase *in vitro* (1, 6). An *E. coli fre* mutant is more susceptible to hydroxyurea, a scavenger of the Tyr^{122} radical, than the wild-type *E. coli* (7), pointing to the protective role of Fre for the aerobic ribonucleotide reductase *in vivo*. Fre produces reduced flavins that can reduce metal ions, including ferrisiderophores (8), Cob(II-I)alamin (9), and chromate (10). Fre is capable of supplying $FADH_2$ to the $FADH_2$-utilizing monooxygenases (11, 12). Despite these apparent biological functions, the genuine physiological role of Fre remains unclear.

Recently, Ingelman *et al.* (13) reported the crystal structure of Fre with or without bound Rfl, revealing that Fre is similar to members of the ferredoxin:$NADP^+$ reductase family in structure, although the similarities in amino acid sequence between Fre and members of the ferredoxin:$NADP^+$ reductase family are low. The crystal structure shows that Fre is organized into an N-terminal flavin-binding domain and a C-terminal NAD(P)H-binding domain; the secondary structures of the two domains are labeled as F and N, respectively. The most interesting feature is that the loop connecting Fβ5 and Fα1 in the flavin-binding domain that normally interacts with the ADP moiety of FAD in other ferredoxin:$NADP^+$ reductases is exceptionally short in Fre (13). Consequently, although FAD is a bound cofactor in most ferredoxin:$NADP^+$ reductase proteins, all three flavin substrates of Fre do not remain bound (13). Because the crystal structure of the Fre·Rfl complex revealed the interactions between the isoalloxazine ring of Rfl and the flavin-binding domain (12) and because the K_m values of Fre for Rfl, FMN, and FAD are very similar (2), it has been proposed that all three flavins mainly interact with residues of the flavin-binding domain through the isoalloxazine ring. However, direct experimental data are unavailable to support the proposed interactions of Fre with FMN and FAD.

In this report we characterized FAD and FMN binding to Fre. The K_d values of Fre with FAD and FMN were determined. The value with FAD was much smaller than that with FMN or Rfl. Molecular dynamics (MD) simulations of Fre with FAD predicted that the ribityl side chain and the ADP moiety of FAD confer extra stability to the Fre·FAD complex. Experimental data supported the simulation model. Studies on the physiological roles of the high affinity of Fre for FAD revealed that FAD is a preferred substrate and inhibitor of Fre. An *in vivo* model for regulating Fre activities in responding to O_2 supply is proposed.

§ Present address: Kemin Biotechnology, L.C., Des Moines, IA 50317-1100.
‖ Present address: Dept. of Chemistry, University of California, Berkeley, CA 94720-1460.
** To whom correspondence should be addressed: School of Molecular Biosciences, Science Hall 301, Washington State University, Pullman, WA 99164-4234. Tel.: 509-335-2787; Fax: 509-335-1907; E-mail: xun@mail.wsu.edu.

[1] The abbreviations used are: Fre, NAD(P)H:flavin oxidoreductase; Rfl, riboflavin; MD, molecular dynamics; KPi, potassium phosphate; DTT, dithiothreitol; ESI-MS, electrospray ionization mass spectrometry; HPLC, high pressure liquid chromatography.

EXPERIMENTAL PROCEDURES
Materials

All reagents were of the highest purity available and were purchased from Sigma, Aldrich, or Fisher Scientific Co.

Overproduction and Purification of Proteins

HpaB, an FADH$_2$-utilizing 4-hydroxyphenylacetate 3-monooxygenase, was overproduced and purified from *E. coli* BL21(DE3) carrying pES2 (11). Overexpression of the cloned *fre* gene in *E. coli* BL21(DE3)(pES1) and purification of Fre were done primarily as reported previously (11). To ensure Fre of the highest purity, a phenyl-agarose chromatography was added to the previously reported procedures. The ammonium sulfate precipitated proteins were dissolved in 20 mM KPi buffer (pH 7.0) containing 1 mM DTT with 25% saturation of ammonium sulfate and loaded onto a phenyl-agarose (Sigma) column (1.5 × 12.5 cm) equilibrated with the same buffer. The proteins were eluted with a linear gradient of ammonium sulfate (25% to 0%, 200 ml) in KPi buffer with 1 mM DTT at a flow rate of 1 ml·min^{-1}. Active fractions eluted with ~10% saturation of ammonium sulfate were pooled together and dialyzed against several changes of 20 mM KPi buffer (pH 7.0) with 1 mM DTT overnight. The sample was then purified by going through a Bioscale Q column and Superdex 75 column as reported previously (11). Purified protein was analyzed by SDS-PAGE (14).

Mass Spectrometry of Fre

ESI-MS was done with a Waters Micromass ZQ mass spectrometer. Fre samples in 10 mM Tris-HCl buffer (pH 7.5) were acidified with formic acid to a final concentration of 0.1% (v/v) and infused into the electrospray ionization source at a flow rate of 10 μl·min^{-1}. The electrospray ionization source temperature and the desolvation temperature were maintained at 90 °C and 150 °C, respectively. The capillary voltage and the cone voltage were 3400 V and 35 V, respectively. Spectra were scanned from m/z 800 to 3000 at a rate of 1 scan/s. Protein mass spectrum was deconvoluted using the MaxEnt software (Waters).

Enzyme Assays

NAD(P)H:flavin oxidoreductase activity was determined spectrophotometrically by monitoring the oxidation of NADH (ϵ_{340} = 6220 M^{-1}·cm^{-1}) in 20 mM KPi buffer (pH 7.0) containing 450 μM NADH and 10 μM FMN or FAD at 30 °C. One unit of NAD(P)H:flavin oxidoreductase activity was defined as the oxidation of 1 nmol NADH/min. A Fre-HpaB coupled assay was performed with 50 nM Fre and 10 μM HpaB in 20 μl of 20 mM KPi buffer (pH 7.0) containing 80 μM NADH and 500 μM 4-hydroxyphenylacetate, with either 5 μM each of FAD and FMN or only 5 μM FAD. The reaction was incubated at 30 °C for 30 min, and the amount of 3,4-dihydroxyphenylacetate produced was measured by a previously reported HPLC method (11).

HPLC Analysis of Fre

A HPLC system equipped with a photodiode array detector (Waters) and a Biosep Sec-S3000 size-exclusion column (7.8 × 300 mm; Phenomenex) was used to estimate the fraction of Fre molecules that contained tightly bound flavins. Pure Fre (200 μg) was eluted from the column with an isocratic flow of 20 mM KPi (pH 7.0) buffer with 1 mM DTT at 0.5 ml·min^{-1}. The amount of flavin co-eluted with Fre was estimated by comparing the elution peak area of Fre derived at 450 nm with the elution peak area of free flavin standards. The same HPLC system equipped with a Delta Pak C$_{18}$-300Å reverse phase column (3.9 × 150 mm; Waters) was used to determine the nature of the tightly bound flavin. Fre sample (80 μg) was eluted from the column with a 33-ml linear gradient of acetonitrile in 0.1% trifluoroacetic acid (0–70%) with a flow rate of 1 ml·min^{-1}. Retention time of the flavin dissociated from Fre was compared with those of free flavin standards.

Measurement of the Dissociation Constant

The dissociation constants, K_d, of the Fre·FAD and Fre·FMN complexes were determined by a spectrofluorometric titration method using a spectrofluorometer (Jobin Ybon Fluorlog). A 48 μM Fre solution in 20 mM KPi buffer (pH 7.4) was titrated with various amounts of flavin added from a 50 μM stock solution, and the change in fluorescence after each addition of flavin was recorded. The excitation wavelength was set at 280 nm, and fluorescence emission of Fre was recorded from 300 to 400 nm at 5-nm intervals. Both excitation and emission monochromator slit widths were set at 5 nm. The fluorescence intensity of Fre was plotted against the ratio of initial concentration of FAD to Fre and fitted with the following equation

$$I_{\text{fit}} = \kappa(I_0[Fre]_0 + x[I_0 - I_1]) \qquad \text{(Eq. 1)}$$

in which κ is a scaling constant to compare the model with experimental data, I_0 is the fluorescence intensity of Fre, $[Fre]_0$ is the initial concentration of Fre at that titration point, I_1 is the fluorescence intensity of the Fre·FAD complex, and x is the final concentration of the Fre·FAD complex. The value of x is calculated by the following equation.

$$x = \frac{([Fre]_0 + [FAD]_0 + K_d) - \sqrt{([Fre]_0 + [FAD]_0 + K_d)^2 - 4[Fre]_0[FAD]_0}}{2}$$
$$\text{(Eq. 2)}$$

The effect of AMP on the K_d of Fre for FAD was also determined. The experimental setup was identical to that described above, except that 0.18 mM AMP was included in the solution.

MD Simulations

The initial geometries of the Fre·FAD and Fre·FMN complexes were based on the crystal structure of the Fre·Rfl complex (from Dr. Vincent Nivière of the Université Joseph Fourier). The complete protein sequence was reconstituted and annealed by MD simulations using the package GROMACS (15, 16) running on a dual-CPU Linux work station. MD simulations were performed in the presence of 4895 water molecules of simple point charge as solvent. Periodical conditions were imposed for the triclinic simulation box. The GROMOS-96 43a1 force field was used for the Fre·FMN simulation, whereas the GROMACS force field was used for the Fre·FAD simulation. After the initial energy minimization and subsequent relaxation runs, the system was allowed to further equilibrate for another 800 ps with Berendsen-type temperature (300 K) and pressure (1.0 atm) coupling to an external bath.

MD Trajectory Analysis

Hydrogen Bonding—A 1-ns trajectory was recorded for each of the Fre·FAD and Fre·FMN runs. Hydrogen bonding analyses between Fre and the flavin substrate were performed. A hydrogen bond is registered when the distance between the hydrogen bonding donor (OH and NH) and acceptor (O: and N:) is less than 0.25 nm.

Representative Structure—Root mean square deviation clustering analysis was performed every 5 ps along the trajectory to locate the representative structure for the complexes. In the full-linkage clustering algorithm, a structure is added to the existing cluster when its distance to any element of the cluster is less than the 0.1-nm cutoff. The 5-ps structures were categorized according to their root mean square deviation values. A structure from the middle of the root mean square deviation distribution was extracted from the MD trajectory as the representative configuration.

Kinetic Analysis of Fre

The inhibitory effects of FAD on Fre activity were examined in the presence of NADPH and FMN. Reciprocal initial velocities were plotted against the reciprocal substrate (NADPH or FMN) concentrations at various fixed concentrations of FAD to determine the nature of the inhibitions. Inhibition constants were then determined from the Michaelis-Menten plots fitted with Equation 3 (for competitive inhibition) and Equation 4 (for mixed inhibition)

$$V_o = \frac{V_{\text{max}}[S]}{K_M\left(1 + \dfrac{[I]}{K_i}\right) + [S]} \qquad \text{(Eq. 3)}$$

$$V_o = \frac{V_{\text{max}}[S]}{K_M\left(1 + \dfrac{[I]}{K_i}\right) + \left(1 + \dfrac{[I]}{K_i'}\right)[S]} \qquad \text{(Eq. 4)}$$

using the GraFit 5.0 program (Erithacus Software Ltd.). The apparent kinetic parameters of Fre for the NADPH-FMN substrate pair were also determined from Michaelis-Menten plots fitted with the following equation

$$V_o = \frac{V_{\text{max}}[S]}{K_M + [S]} \qquad \text{(Eq. 5)}$$

using the GraFit program.

RESULTS

Purity of Fre Preparation—Forty-five mg of Fre was purified from 289 mg of protein in the cell extracts. The protein was
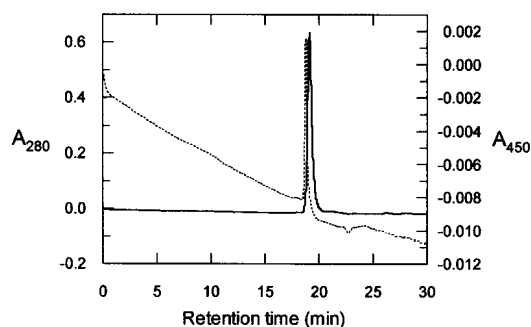
FIG. 1. **HPLC analysis of Fre by a size-exclusion column.** Fre sample (200 μg) was eluted from the column with an isocratic flow of 20 mM KPi buffer (pH 7.0) plus 1 mM DTT. Absorptions at 280 nm (*solid line,* Fre) and at 450 nm (*dashed line,* flavins) were recorded by the photodiode array detector. The area of the 450 nm peak that co-eluted with Fre was compared with that of a known amount of FMN standard quantified at 450 nm.

FIG. 2. **HPLC analysis of Fre by a C$_{18}$ reverse phase column.** Fre sample (80 μg) was eluted from the column with a 33-ml linear gradient of acetonitrile in 0.1% trifluoroacetic acid (0–70%) with a flow rate of 1 ml·min^{-1}. A minor peak with maximal absorption at 450 nm (*dashed line*) was eluted from the column at 9.938 min, whereas a major peak with maximal absorption at 280 nm (*solid line*) was eluted from the column at 26.0 min. *Inset,* absorption spectrum of the 9.938-min peak with maximal absorptions at 372 and 450 nm.

purified to apparent homogeneity. The purified Fre was acidified and analyzed by ESI-MS; the molecular weight of Fre was determined to be 26,115 ± 5, which is practically identical to Fre's theoretical molecular weight of 26,111 calculated from the amino acid sequence. No other major molecular mass was detected by ESI-MS, further validating the purity of the Fre preparation. The purified Fre had a specific activity of 69,230 ± 295 units·mg^{-1} when reducing FMN with NADH as the electron donor at 30 °C. The highly concentrated and pure Fre had a pale yellow color, suggesting the possibility of flavins being bound to Fre. The specific flavin bound to Fre was further tested.

HPLC Analyses of Fre—When 200 μg (~8 nmol) of Fre was loaded onto an HPLC size-exclusion column, we detected a small amount of flavin co-eluted with the Fre based on the absorption spectrum recorded by the photodiode array detector (Fig. 1). The flavin peak was centered at the beginning of the protein peak, consistent with the slightly larger molecular weight of the Fre·flavin complex as compared with that of Fre alone. After integrating the peak area of the flavin peak that co-eluted with Fre and comparing it with the peak area of free FMN standards, our data showed that ~0.13 nmol equivalent of FMN was co-eluted with Fre. When Fre was loaded onto a C$_{18}$ reverse phase HPLC column, the Fre-bound flavin was dissociated from the protein, with a retention time of 9.938 min (Fig. 2). A typical absorption spectrum of a flavin molecule was clearly detected (Fig. 2, *inset*). The respective retention times of free FAD, FMN, and Rfl standards were 9.985, 10.155, and 10.898 min, suggesting that the Fre-bound flavin is possibly FAD. This possibility was further examined by loading 25 μl of a mixture of Fre (0.14 μM) with either FMN or FAD (0.24 μM) onto the HPLC size-exclusion column. About 25% of FAD in the Fre-FAD mixture was co-eluted with Fre, but only 2.2% of FMN in the Fre-FMN mixture was co-eluted with Fre.

Dissociation Constants for FAD and FMN—Aliquots of FAD solution were added to a 48 μM Fre solution in 20 mM KPi (pH 7.4) buffer. The binding of FAD to Fre quenched the fluorescence of Fre, resulting in a gradual decrease in the fluorescence intensity of Fre (Fig. 3, *inset*). The K_d for FAD was determined to be 29 ± 9 nM after plotting the fluorescence intensity of Fre against the ratio of the added FAD concentration to the initial Fre concentration (Fig. 3). Using a similar methodology, the K_d for FMN was determined to be 1.5 ± 0.2 μM.

Computer Modeling of Fre·FAD Complex—The low K_d value for FAD is not consistent with the previous hypothesis that the isoalloxazine rings of the flavin substrates provide the major determinant for the binding of the three flavins to Fre and that the flavins have similar affinity for Fre (13). We hypothesized
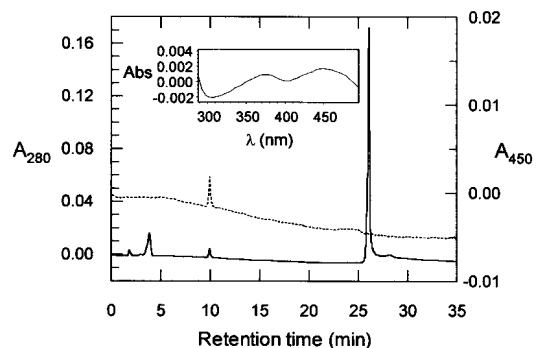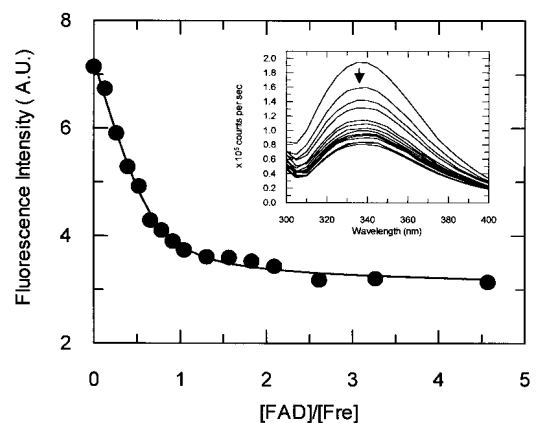

FIG. 3. **Fluorescence quenching titration of Fre by FAD.** The change in fluorescence of Fre, due to the sequential additions of FAD (from a 50 μM stock) and the binding of FAD to Fre, was plotted against the concentration ratio of FAD to Fre. The *filled circle* represents the average of three independent titrations, and the *solid black line* represents the best-fitted titration curve for Equation 1 (see "Experimental Procedures"). The K_d was calculated from the best-fitted curve as 29 nM. *Inset,* the decrease in the fluorescence of Fre after each addition of FAD to the Fre solution.

that the ribityl moiety and the ADP moiety of FAD might interact with other structural elements in Fre and provide extra stability for the Fre·FAD complex. To test this hypothesis, the structure of the Fre·FAD complex was modeled by MD simulations. MD simulations showed that FAD could adopt an unusual bent conformation (Fig. 4*A*). Amino acid residues located in the loop connecting Fβ5 and Fα1 in the flavin-binding domain (*e.g.* Gly[65] and Asn[70]) and at the proposed NAD(P)H-binding site (*e.g.* Thr[112], Gln[143], and Arg[202]) were shown to form additional H-bonding with the ribityl side chain and the ADP moiety of FAD (Fig. 4*B*). Specifically, the MD trajectory showed that there were 8.03 ± 2.13 (3,600 (average) 0.5-ps snapshots of a 900-ns trajectory with S.D.) hydrogen bonds between the Fre protein matrix and the FAD substrate, whereas there were only 4.75 ± 1.72 hydrogen bonds between Fre and FMN. The number of hydrogen bonds appeared to vary with time, reflecting the dynamic nature of the Fre·FAD complex. This is illustrated in Fig. 4*B*, in which we show two snapshots of the hydrogen-bonding network around FAD.

Inhibitory Effect of FAD on Fre—The computer modeling of the Fre·FAD complex suggested that the ADP moiety of FAD interacts dynamically with amino acid residues located at the proposed NAD(P)H-binding site. This hypothesis was further
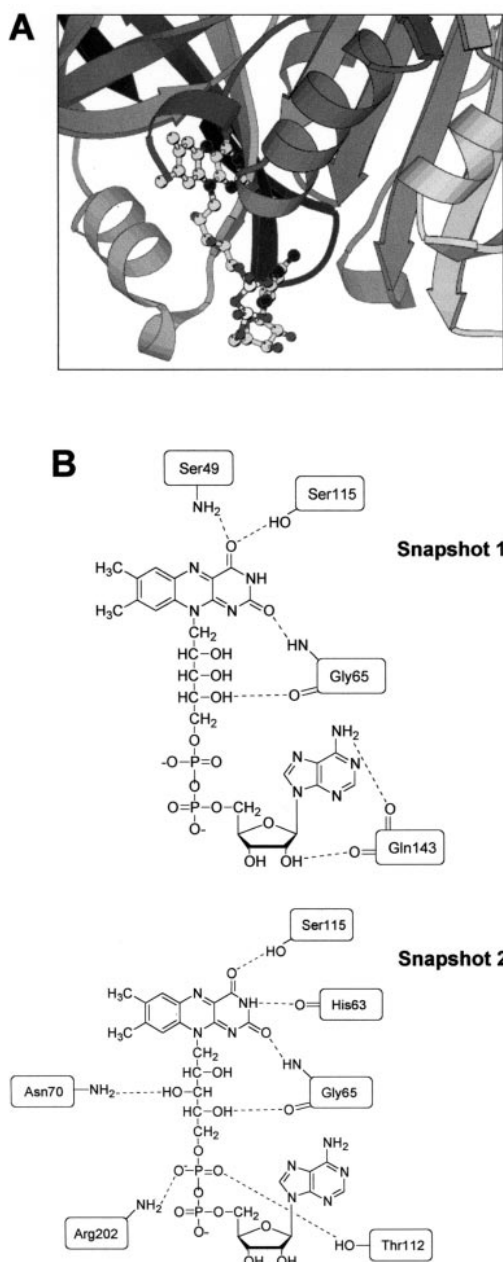
A, ribbon representation of the Fre·FAD complex from the MD
simulations. The FAD molecule in the unique bent conformation is
represented as a *ball-and-stick model*. The schematic was created with
the MOLSCRIPT program (27). **B**, two snapshots of the H-bonding
networks around the FAD molecule from the MD simulations.

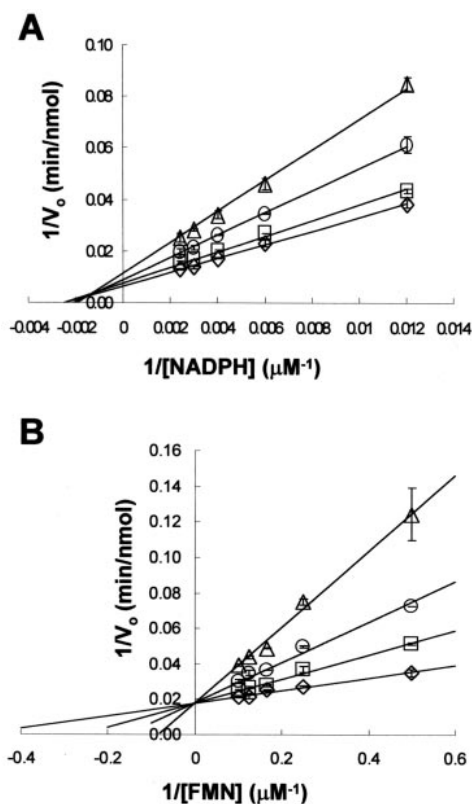Fig. 4. **Computer modeling of Fre·FAD complex by MD simu-
lations.**

Fig. 5. **Inhibition of Fre activity by FAD when NADPH was
used as the electron donor.** *A*, FAD was a mixed-type inhibitor with
respect to NADPH. Fre (2.4 μg) activity was assayed as a function of
NADPH concentrations (83, 166, 249, 332, and 415 μM) using 10 μM
FMN in the absence ($\diamond$) and presence of 100 ($\square$), 250 ($\bigcirc$), and 500 ($\triangle$)
nM FAD. *B*, FAD was a competitive inhibitor with respect to FMN. Fre
(2.4 μg) activity was assayed as a function of FMN concentrations (2, 4,
6, 8, and 10 μM) using 200 μM NADPH in the absence ($\diamond$) and presence
of 100 ($\square$), 250 ($\bigcirc$), and 500 ($\triangle$) nM FAD. All of the rate measurements
are mean of triplicate $\pm$ S.D.

examined. The K_d value for FAD was determined to be 83 $\pm$ 25
nM in the presence of 0.18 mM AMP, a known competitive
inhibitor of Fre with respect to NAD(P)H (with reported K_i
values ranging from 0.3 to 0.5 mM) (2, 5). This K_d value is
almost 3 times larger than the K_d value determined in the
absence of AMP.

The effect of FAD as an inhibitor for Fre activity was studied
using NADPH as the electron donor and FMN as the major
electron acceptor. It has been reported that the $K_{m,NADPH}$ of
Fre is 14,000 μM with a k_{cat} of 16 s^{-1} if FAD is the sole electron
acceptor (5). Because the highest concentration of NADPH used
in our inhibitory study was 415 μM, Fre did not have any
detectable activity for FAD reduction due to the large
$K_{m,NADPH}$ value. Because FAD was practically not a substrate
for Fre under the assay conditions, its inhibitory effect on FMN

reduction with NADPH was studied. Fre activity was deter-
mined as a function of NADPH concentration (83–415 μM) in
the presence of a fixed concentration of FMN (10 μM) at several
concentrations of FAD. The double-reciprocal plots showed a
series of lines converged at a point to the left of the *y* axis (Fig.
5*A*), indicating that FAD is a mixed-type inhibitor with respect
to NADPH with a K_i of 0.43 $\pm$ 0.07 μM and a K_i' of 0.59 $\pm$ 0.17
μM; the apparent $K_{m,NADPH}$ was 418 $\pm$ 41 μM. When Fre activ-
ity was determined as a function of FMN concentration (2–10
μM) in the presence of a fixed concentration of NADPH (200 μM)
at several concentrations of FAD, FAD exhibited a typical
competitive inhibition effect (Fig 5*B*), with a K_i of 0.10 $\pm$ 0.01
μM and an apparent $K_{m,FMN}$ of 2.0 $\pm$ 0.2 μM.

The effect of FAD on the activity of Fre for FMN reduction
with NADH as the electron donor was also studied. Because
FAD reduction by Fre is much slower than FMN reduction
when NADH is less than 100 μM (5), the effect of FAD was
studied by measuring the Fre activity under a fixed concentra-
tion of NADH (80 μM) and FMN (10 μM), with various FAD
concentrations. FAD at 1 μM reduced the rate of NADH con-
sumption of Fre by 13%, and at 10 μM, FAD reduced the rate by
45% (Fig. 6). The decrease was shown to be due to the prefer-
ential reduction of FAD when the amount of produced FADH$_2$
was measured by HpaB, an FADH$_2$-utilizing 4-hydroxypheny-
lacetate 3-monooxygenase that does not use FMNH$_2$ (11).
HpaB was used in excess to ensure ultimate usage of FADH$_2$
produced in the assay. After a 30-min incubation, 1.6 nmol of
NADH was consumed, and 1.7 $\pm$ 0.1 nmol (average of three
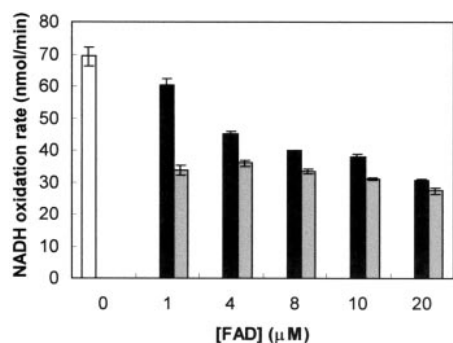samples $\pm$ S.D.) of 3,4-dihydroxyphenylacetate was produced

FIG. 6. **Inhibition of Fre activity by FAD when NADH was used as the electron donor.** Fre (1.0 μg) activity was assayed in the presence of a fixed concentration of NADH (80 μM) with 10 μM FMN alone ($\square$), 10 μM FMN with various concentrations of FAD ($\blacksquare$), and FAD alone ($\blacksquare$) in 1 ml of 20 mM KPi buffer (pH 7.0). All of the rate measurements are mean of triplicate $\pm$ S.D.

with FAD alone in the assay; whereas 1.4 $\pm$ 0.1 nmol of the product was formed in the presence of equal concentrations of FMN and FAD. Therefore, about 82% of the NADH was used to reduce FAD under the assay conditions containing 5 μM each of FAD and FMN, with the remainder used for FMN reduction.

DISCUSSION

Fre had a much higher affinity for FAD than for FMN. The K_d value for the Fre·FAD complex (29 $\pm$ 9 nM) was 52 times lower than that of FMN (1.5 $\pm$ 0.2 μM). The K_d values for Rfl and lumichrome, a flavin analog, are 3.6 and 0.5 μM (17, 18). Thus, among its flavin substrates, Fre binds FAD the most tightly. The tight binding was also observed by the co-elution of FAD with Fre from the HPLC size-exclusion chromatography (Fig. 1). Results of the MD simulations (Fig. 4A) showed that not only the isoalloxazine ring of FAD but also the ribityl side chain and the ADP moiety were involved in binding to Fre, offering theoretical support for tighter binding for FAD than for FMN of Rfl. On the basis of the crystallized Fre·Rfl structure, which shows only one direct H-bond from the 2'-OH of the ribityl side chain to the carbonyl oxygen of Pro[47] (on Fβ4) (13), and the similar K_m values for Rfl, FMN, and FAD, it has been hypothesized that Fre binds Rfl, FMN, and FAD mainly through the isoalloxazine ring (1, 13). The proposed interaction is real for Rfl and FMN, but not for FAD. The MD simulations predicted the formation of 3.28 extra H-bonds on average from the ribityl side chain and ADP moiety of FAD with Fre (Fig. 4B). Considering the energy of a typical H-bond to be 2.9–7.2 kcal/mol (19), the extra H-bonds in the Fre·FAD complex contribute to a significant stabilization energy (enthalpy) of 9.5–23.6 kcal/mol, in comparison with the Fre·FMN complex. This stabilization energy should be viewed as an upper bound, because entropy (*e.g.* the bent conformation and larger size of the FAD can increase the entropy of the Fre·FAD complex) will reduce the stabilization. This view is consistent with the extra stabilization energy (free energy) of 2.3 kcal/mol calculated from the determined K_d values of the Fre·FAD complex relative to the Fre·FMN complex.

The bent conformation of FAD predicted by MD simulations is similar to the conformation adopted by the FAD prosthetic group in the *E. coli* flavodoxin reductase, in which FAD exhibits a U-shaped conformation (20). Interestingly, the flavodoxin reductase also lacks a full-size adenosine-interacting loop connecting Fβ5 and Fα1, as does Fre. Structure-based sequence alignment of Fre with the flavodoxin reductase shows that two flavodoxin reductase residues that H-bond with the ribityl side chain and the adenine ring of the FAD prosthetic group (Arg[50] and Thr[116]) are conserved in Fre (Arg[46] and Thr[112]) (13, 20). The hydrogen bonding of Thr[112] with FAD is captured by snap-

shot of MD simulations (Fig. 4), whereas the dynamic interaction of Arg[46] with FAD is not presented in the snapshot. The flavodoxin reductase has a Trp[248] residue at the C terminus, which provides additional interaction with the adenine ring of FAD. Such a Trp residue is not present in the Fre C terminus and may partly explain why Fre does not bind FAD permanently, whereas the flavodoxin reductase does.

Unlike the experimentally verified flavin-binding site, the NAD(P)H-binding site of Fre is only a proposed model (13) based on comparisons with different ferredoxin:NADP$^+$ reductase·AMP complexes (21, 22). The adenine ring and the ribose group of the 2'-phospho-ADP moiety of NADPH are proposed to bind to Fre near the amino ends of the α-helices of the NAD(P)H-binding domain, and Arg[202] and His[144] may bind the pyrophosphate group of NAD(P)H (13). Interestingly, our MD simulations also predicted amino acid residues at these regions, such as Gln[143] and Arg[202], to form H-bonds with the ADP moiety of FAD (Fig. 4B). The overlapping binding sites of FAD and NAD(P)H were supported by several lines of results. Firstly, 0.18 mM AMP, a known competitive inhibitor with respect to the NAD(P)H (2, 5), increased the K_d value of the Fre·FAD complex from 29 nM to 83 nM. In comparison, NADP$^+$ or 3-aminopyridine adenosine dinucleotide phosphate, an NADPH analog, has no effect on the K_d of Fre for Rfl (18). AMP affects the binding of FAD to Fre probably by competing with the ADP moiety of FAD for the NAD(P)H-binding site, leading to an increased K_d.

Secondly, kinetic analysis showed that FAD behaves as a competitive inhibitor with respect to FMN and a mixed-type inhibitor with respect to NADPH (Fig. 5). Competitive inhibition of FAD upon FMN is expected because FAD should compete with FMN for the flavin-binding site. However, the mixed-type inhibition upon NADPH supports the MD simulation model. Lumichrome, an Fre-competitive inhibitor with respect to Rfl, is an uncompetitive inhibitor with respect to NADPH (2). Hence, lumichrome does not inhibit the formation of Fre·NADPH complex. The interactions between the ADP moiety of FAD and residues at the NAD(P)H-binding site may inhibit the formation of Fre·NADPH complex, leading to the observed mixed-type inhibitory effect.

The bent conformation of FAD also provides a plausible explanation for the extremely large $K_{m,NADH}$ (301 μM) and $K_{m,NADPH}$ (14,000 μM) values during FAD reduction, in comparison with the corresponding K_m values for Rfl and FMN reduction (1, 2, 5). Because FAD binds tightly to Fre through both the isoalloxazine ring and the ADP moiety (Fig. 4), NADH has to compete with the ADP moiety of FAD for the binding site. Consequently, a higher concentration of NADH is required to outcompete the ADP moiety of FAD for the NAD(P)H-binding site, leading to a larger $K_{m,NADH}$ value than that for Rfl and FMN reduction. In the bent conformation, the negatively charged pyrophosphate group of FAD is also located in close proximity to the proposed binding site for the 2'-phosphate group of NADPH (13) (Fig. 4A). The highly negatively charged pyrophosphate group may destabilize the binding of NADPH through repulsion with the negatively charged 2'-phosphate group of NADPH. Thus, the $K_{m,NADPH}$ value is 46 times larger than the $K_{m,NADH}$ when FAD is the electron acceptor. The single phosphate group of FMN may also destabilize NADPH binding to Fre by the same mechanism, resulting in a $K_{m,NADPH}$ of 418 $\pm$ 41 μM (calculated from Fig. 5); whereas the $K_{m,NADH}$ is merely 14.9 $\pm$ 0.8 μM during FMN reduction (data not shown).

The high affinity of Fre for FAD may imply that the *in vivo* Fre activity is much lower than previously expected under aerobic conditions. NADH and NADPH concentrations inside

aerobically growing *E. coli* have been reported in the range of 20 and 150 μM, respectively (23). Intracellular free Rfl, FMN, and FAD concentrations have not been clearly defined. Only one study reports the internal free FAD concentration of *Amphibacillus xylanus* to be 13 μM (24). Intracellular Rfl concentration should be much lower than those of FMN and FAD because Rfl should be transformed into the coenzyme forms FMN and FAD in order to fulfill its metabolic purpose (25). Assuming the internal free FMN and FAD concentrations to be in the order of ~10 μM, then *in vivo* Fre activity should be mainly due to the preferential reduction of FAD by NADH as demonstrated by our *in vitro* assay (Fig. 6) and the Fre-HpaB coupled assay. Fre literally cannot use NADPH to reduce FAD *in vivo* because the $K_{m,NADPH}$ value is much higher than the internal NADPH concentration. Thus, the *in vivo* Fre activity should be suppressed due to the low internal NADH concentration in comparison with the $K_{m,NADH}$ value. The low *in vivo* Fre activity is advantageous to the organism because this prevents unrestrained production of $FADH_2$, wasteful reoxidation of the labile $FADH_2$, and excessive production of detrimental reactive oxygen species such as H_2O_2 (26).

In summary, this study demonstrated that FAD binds more tightly to Fre than either FMN or Rfl does. The tight binding likely makes FAD the preferred substrate under *in vivo* conditions (Fig. 6). Experimental data and MD simulations suggested that the tight binding is due to an unusual bent conformation of FAD, allowing additional interactions between FAD and Fre. The ADP moiety of FAD likely competes with NAD(P)H for binding to Fre, explaining the large K_m values for NADH and NADPH during FAD reduction. *E. coli* is a facultative anaerobe, growing both aerobically and anaerobically. When *E. coli* grows with sufficient O_2 supply, the intracellular NADH concentration is about 20 μM, or 2% of total NADH and NAD^+ (23). The low NADH concentration supports very low Fre activity for FAD reduction, and FAD also inhibits FMN reduction by Fre. Thus, our data suggest that Fre activities are likely suppressed in aerobically growing *E. coli* cells.

REFERENCES

1. Fontecave, M., Eliasson, R., and Reichard, P. (1987) *J. Biol. Chem.* **262,** 12325–12331
2. Fieschi, F., Nivière, V., Frier, C., Decout, J.-L., and Fontecave, M. (1995) *J. Biol. Chem.* **270,** 30392–30400
3. Inouye, S. (1994) *FEBS Lett.* **347,** 163–168
4. Lei, B., Liu, M., Huang, S., and Tu, S. C. (1994) *J. Bacteriol.* **176,** 3552–3558
5. Nivière, V., Fieschi, F., Decout, J.-L., and Fontecave, M. (1999) *J. Biol. Chem.* **274,** 18252–18260
6. Fontecave, M., Eliasson, R., and Reichard, P. (1989) *J. Biol. Chem.* **264,** 9164–9170
7. Covès, J., Nivière, V., Eschenbrenner, M., and Fontecave, M. (1993) *J. Biol. Chem.* **268,** 18604–18609
8. Covès, J., and Fontecave, M. (1993) *Eur. J. Biochem.* **211,** 635–641
9. Fonseca, M., and Escalante-Semerena, J. C. (2000) *J. Bacteriol.* **182,** 4304–4309
10. Puzon, G. J., Petersen, J. N., Roberts, A. G., Kramer, D. M., and Xun, L. (2002) *Biochem. Biophys. Res. Commun.* **294,** 76–81
11. Xun, L., and Sandvik, E. R. (2000) *Appl. Environ. Microbiol.* **66,** 481–486
12. Louie, T. M., Webster, C. M., and Xun, L. (2002) *J. Bacteriol.* **184,** 3492–3500
13. Ingelman, M., Ramaswamy, S., Nivière, V., Fontecave, M., and Eklund, H. (1999) *Biochemistry* **38,** 7040–7049
14. Laemmli, U. K. (1970) *Nature* **227,** 680–685
15. Berendsen, H. J. C., van der Spoel, D., and van Drunen, R. (1995) *Comput. Phys. Commun.* **91,** 43–56
16. Lindahl, E., Hess, B., and van der Spoel, D. (2001) *J. Mol. Model.* **7,** 306–317
17. Nivière, V., Fieschi, F., Decout, J.-L., and Fontecave, M. (1996) *J. Biol. Chem.* **271,** 16656–16661
18. Nivière, V., Vanoni, M. A., Zanetti, G., and Fontecave, M. (1998) *Biochemistry* **37,** 11879–11887
19. Voet, D., and Voet, J. G. (1995) *Biochemistry*, 2nd Ed., p. 176, John Wiley & Sons, New York
20. Ingelman, M., Bianchi, V., and Eklund, H. (1997) *J. Mol. Biol.* **268,** 147–157
21. Serre, L., Vellieux, F. M., Medina, M., Gomez-Moreno, C., Fontecilla-Camps, J. C., and Frey, M. (1996) *J. Mol. Biol.* **263,** 20–39
22. Karplus, P. A., Daniels, M. J., and Herriott, J. R. (1991) *Science* **251,** 60–66
23. Penfound, T., and Foster, J. W. (1996) in *Escherichia coli and Salmonella Cellular and Molecular Biology* (Neidhardt, F. C., ed), pp. 721–730, ASM Press, Washington, D. C.
24. Ohnishi, K., Nimura, Y., Yokoyama, K., Hidaka, M., Masaki, H., Uchimura, T., Suzuki, H., Uozumi, T., Kozaki, M., Komagata, K., and Nishino, T. (1994) *J. Biol. Chem.* **269,** 31418–31423
25. Bacher, A., Eberhardt, S., and Richter, G. (1996) in *Escherichia coli and Salmonella Cellular and Molecular Biology* (Neidhardt, F. C., ed), pp. 657–664, ASM Press, Washington, D. C.
26. Gibson, Q. H., and Hastings, J. W. (1962) *Biochem. J.* **83,** 368–377
27. Kraulis, P. (1991) *J. Appl. Crystallogr.* **24,** 946–950